2-15-2017

A Novel Electrochemical Biosensor Based On Fe3O4 Nanoparticles-Polyvinyl Alcohol Composite for Sensitive Detection of Glucose

Niuosha Sanaeifar
Amirkabir University of Technology

Mohammad Rabiee
Amirkabir University of Technology

Mojgan Abdolrahim
Amirkabir University of Technology

Mohammadreza Tahriri
Amirkabir University of Technology

Daryoosh Vashaee
North Carolina State University

See next page for additional authors

Accepted version. *Analytical Biochemistry,* Vol. 519 (February 15, 2017): 19-26. DOI.

Authors
Niuosha Sanaeifar, Mohammad Rabiee, Mojgan Abdolrahim, Mohammadreza Tahriri, Daryoosh Vashaee, and Lobat Tayebi

A Novel Electrochemical Biosensor Based on Fe_3O_4 Nanoparticles-polyvinyl Alcohol Composite for Sensitive Detection of Glucose

Niuosha Sanaeifar
Biomaterial Group, Faculty of Biomedical Engineering, Amirkabir University of Technology, Tehran, Iran
Mohammad Rabiee
Biomaterial Group, Faculty of Biomedical Engineering, Amirkabir University of Technology, Tehran, Iran
Mojgan Abdolrahim
Biomaterial Group, Faculty of Biomedical Engineering, Amirkabir University of Technology, Tehran, Iran
Mohammadreza Tahriri
Biomaterial Group, Faculty of Biomedical Engineering, Amirkabir University of Technology, Tehran, Iran
School of Dentistry, Marquette University
Milwaukee, WI
Daryoosh Vashaee
Electrical and Computer Engineering Department, North Carolina State University, Raleigh, NC

Analytical Biochemistry, Vol. 519 (February 15, 2017): pg. 19-26. DOI.

Lobat Tayebi
School of Dentistry, Marquette University
Milwaukee, WI
Department of Engineering Science, University of Oxford, Oxford, UK

Abstract: In this research, a new electrochemical biosensor was constructed for the glucose detection. Iron oxide nanoparticles (Fe_3O_4) were synthesized through co-precipitation method. Polyvinyl alcohol-Fe_3O_4 nanocomposite was prepared by dispersing synthesized nanoparticles in the polyvinyl alcohol (PVA) solution. Glucose oxidase (GOx) was immobilized on the PVA-Fe_3O_4 nanocomposite via physical adsorption. The mixture of PVA, Fe_3O_4 nanoparticles and GOx was drop cast on a tin (Sn) electrode surface (GOx/PVA-Fe_3O_4/Sn). The Fe_3O_4 nanoparticles were characterized by X-ray diffraction (XRD). Also, Fourier transform infrared (FTIR) spectroscopy and field emission scanning electron microscopy (FE-SEM) techniques were utilized to evaluate the PVA-Fe_3O_4 and GOx/PVA-Fe_3O_4 nanocomposites. The electrochemical performance of the modified biosensor was investigated using electrochemical impedance spectroscopy (EIS) and cyclic voltammetry (CV). Presence of Fe_3O_4 nanoparticles in the PVA matrix enhanced the electron transfer between enzyme and electrode surface and the immobilized GOx showed excellent catalytic characteristic toward glucose. The GOx/PVA-Fe_3O_4/Sn bioelectrode could measure glucose in the range from 5×10^{-3} to 30 mM with a sensitivity of 9.36 μA mM^{-1} and exhibited a lower detection limit of 8 μM at a signal-to-noise ratio of 3. The value of Michaelis-Menten constant (K_M) was calculated as 1.42 mM. The modified biosensor also has good anti-interfering ability during the glucose detection, fast response (10 s), good reproducibility and satisfactory stability. Finally, the results demonstrated that the GOx/PVA-Fe_3O_4/Sn bioelectrode is promising in biosensor construction.

Keywords: Biosensor; Electrochemical; Glucose; Fe_3O_4 nanoparticles; Poly(vinyl alcohol); Electrode

1. Introduction

The accurate detection of glucose concentration is vital in various fields such as biology, biochemistry, clinical chemistry and food analysis. For this aim, glucose biosensor is widely used for determination of glucose in blood and food.[1–5] Between several detection methods, electrochemical biosensors have attracted considerable attention due to their excellent selectivity, simplicity and low cost.[4,6] Electrochemical techniques, particularly amperometric biosensors based on glucose oxidase (GOx) immobilization, which can catalyze the oxidation of glucose, have been widely used in glucose sensing.[7–9]

Different types of nanomaterials with various size, shapes, physical and chemical properties owing to advances in synthetic methodologies are being extensively used in biosensors.[10–16] These materials exhibit significant benefits due to their small size, large surface-to-volume ratio, optical characteristics and high catalytic properties compared to

macroscale materials. Because of their adsorption ability, they are useful for the immobilization of biomolecules such as GOx.[17–20] Moreover, the capability of nanoparticles in electron transfer improvement between electrode and active site of the enzyme make them suitable for applying in enzymatic biosensors applications.[17] Wide variety of metal nanoparticles including gold (Au).[21,22] silver (Ag).[23] palladium (Pd),[24] platinum (Pt)[25,26] and metal oxide[27] nanoparticles have been extensively used to construct different sensors, due to their unique features.[28] In recent years, Fe_3O_4 magnetic nanoparticles have attracted a lot of attention in many fields such as biotechnology, pharmacy, cell separation and drug delivery, owing to their interesting properties including biocompatibility, low toxicity, strong supermagnetism, catalytic activity and the ease of preparation process. These magnetic nanoparticles are appropriate for immobilization of different biomolecules such as enzymes. Therefore, it would be promising to use them in biosensor applications.[29–33] It must be mentioned that, by modifying these nanoparticles, using conductive polymers and biopolymers, can be overcome the problems of aggregation and rapid degradation.[17]

A number of polymers have been used to stabilize the biomolecules in the design of biosensors. Among them, polyvinyl alcohol (PVA) has been widely utilized as a matrix for entrapment of GOx due to its biocompatibility, non-toxicity, water solubility, good chemical and thermal stability. PVA has large numbers of hydroxyl groups, which provides a biocompatible microenvironment.[34,35]

Xin et al. have studied screen-printed carbon electrode modified by Fe_3O_4-Au magnetic nanoparticles coated horseradish peroxidase and graphene sheets-nafion film based hydrogen peroxide biosensor.[36] Godarzi et al. have prepared carbon nanotubes decorated by Fe_3O_4 nanoparticles for highly stable and selective non-enzymatic glucose biosensor.[37] Yang et al. have described core-shell Fe_3O_4-enzyme-polypyrrole nanoparticles for glucose biosensor using potentiometric technique.[38] Tan et al. have prepared PVA/ZnO nanorods composite films for hydrogen peroxide biosensor.[39] Lad et al. have fabricated PVA-silica hybrid films for encapsulation of GOx based glucose biosensor using electrochemical technique.[40] Fang et al. have designed glassy carbon electrode modified by PVA-multiwalled carbon nanotubes–Pt nanoparticles hybrids for non-enzymatic hydrogen peroxide sensor.[41]

In this work, a novel glucose biosensor was presented. It was fabricated by dispersing synthesized Fe_3O_4 nanoparticles in the PVA solution and then GOx was immobilized by physical adsorption in the PVA-Fe_3O_4 nanocomposite, drop cast on a tin (Sn) electrode surface (GOx/PVA-Fe_3O_4/Sn). Finally, the characterization and

electrochemical performance of the modified biosensor were examined and discussed in this paper.

2. Experimental procedures

2.1. Reagents

Ferrous chloride anhydrous ($FeCl_2$) and ferric chloride anhydrous ($FeCl_3$) were products of Sigma–Aldrich. Hydrochloric acid 37% (HCl) was purchased from Scharlau. Sodium hydroxide (NaOH) was bought from Merck. These materials have been used for the synthesis of Fe_3O_4 nanoparticles. PVA (87–89% hydrolyzed, average $M_W = 72000$), D(+)-glucose and GOx (Type VII-S, 250000 U g^{-1}) were obtained from Sigma-Aldrich. Disodium phosphate (Na_2HPO_4) and monopotassium phosphate (KH_2PO_4) were used for preparation of phosphate buffer solution (PBS). All chemicals were used without further purification. Also, distilled water was employed for preparation of all aqueous solution.

2.2. Preparation of Fe_3O_4 nanoparticles

Fe_3O_4 nanoparticles have been synthesized by earlier protocol reported co-precipitation method.[42] 5.2 g (0.03 mol) of $FeCl_3$ and 2.0 g (0.015 mol) of $FeCl_2$ (Fe(II):Fe(III) = 0.5) were dissolved in the aqueous solution containing 0.85 mL of 37% HCl and 25 mL of deoxygenated water with vigorous stirring. The mixed solution of iron salts was added drop-wise into 250 mL of 1.5 M NaOH under vigorous stirring at room temperature. After the complete addition of the cationic solution into alkaline solution, the stirring continued for 30 min to complete the nucleation process and formation of Fe_3O_4 nanoparticles. During the procedure nitrogen gas was bubbling through solution and the measured pH value was between 11 and 12. The black precipitate was separated by centrifugation at 4000 rpm for 15 min and washed three times with deoxygenated water to remove unreacted reagents and salts (The reaction of hydrochloric acid and sodium hydroxide produces salt (NaCl)). To neutralize anionic charge on nanoparticles, 500 mL of 0.01 M HCl then added into the mixture with stirring. The magnetic nanoparticles were separated by centrifugation at 4000 rpm for 15 min and deionized water was added to peptize the synthesized Fe_3O_4 nanoparticles (with concentration of 10 mg mL^{-1}).

2.3. Construction of GOx/PVA-Fe_3O_4/Sn electrode

A PVA (3%) solution was prepared by dissolving 3 g of PVA in 100 mL distilled water under magnetic stirring at 85 °C for 2 h. The solutions of glucose oxidase 1, 2, 4,6 and

8 mg mL^{-1} were prepared in PBS buffer (pH = 7). The optimum concentration of glucose oxidase (4 mg mL^{-1}) was chosen by comparing the current response of 5 GOx/PVA-Fe_3O_4/Sn electrode in the presence of 5 mM glucose concentration, which is described in the results and discussions (section 3.5). All the modified electrodes reported in this study were prepared by 4 mg mL^{-1} glucose oxidase. 100 μL Fe_3O_4 nanoparticles in deionized water (10 mg mL^{-1}) was dispersed in 500 μL PVA solution by vigorous stirring at room temperature. As a result, suspension consisting of PVA and dispersed Fe_3O_4 nanoparticles was obtained. Resulting solution and 250 μL of prepared GOx solution was slowly mixed for 1 min. Subsequently, 10 μL of this mixture was drop cast on the surface of the Sn electrode and then dried in air at room temperature to fabricate GOx/PVA-Fe_3O_4/Sn electrode.

2.4. Apparatus and measurements

X-ray diffraction (XRD) (Co-Kα, Philips) was used to investigate the crystalline structure of Fe_3O_4 nanoparticles and the average crystallite size of Fe_3O_4 nanoparticles were calculated using PANalytical X'Pert HighScore software according to Scherrer equation. The PVA-Fe_3O_4 and its interaction with GOx were characterized by Fourier transform infrared (FTIR) spectrophotometer (Nicolet, NEXUS 670). Field emission scanning electron microscopy (FE-SEM) (TESCAN, Mira 3-XMU) was used to study the surface morphology of the prepared nanocomposite films. Electrochemical impedance spectroscopy (EIS) was performed on PVA/Sn, PVA-Fe_3O_4/Sn electrode and GOx/PVA-Fe_3O_4/Sn bioelectrode with 4 mg mL^{-1} GOx in the absence of glucose in the frequency range, 0.01–10^5 Hz. Cyclic voltammetry (CV) of PVA/Sn film, PVA-Fe_3O_4/Sn electrode and GOx/PVA-Fe_3O_4/Sn bioelectrode with 4 mg mL^{-1} GOx were investigated between −0.9 and 0.7 V with the scan rate of 50 mVs^{-1}. All electrochemical measurements were carried out on an Autolab Potentiostat/Galvanostat at room temperature in PBS buffer (pH = 7) solution, utilizing three-electrode system with a Sn electrode as working electrode, a Pt wire as auxiliary electrode and an Ag/AgCl electrode as reference.

3. Results and discussion

3.1. Characterization of Fe_3O_4 nanoparticles, PVA-Fe_3O_4 nanocomposite and GOx/PVA-Fe_3O_4/Sn electrode

Fig. 1 shows the XRD pattern of the synthesized Fe_3O_4 nanoparticles. The 2θ values of the Fe_3O_4 nanoparticle 21.3°, 34.9°, 41.5°, 50.3°, 62.6°, 67.0°, and 73.8° correspond to the crystal planes of (111), (220), (311), (400), (422), (511) and (440), respectively, which is

quite similar to that reported before for magnetite nanoparticles.[43] The reflection planes are broad, indicating the nanosize of the synthesized Fe_3O_4 particles. No peaks of impurities are observed in XRD pattern, revealing the high purity of the Fe_3O_4 nanoparticles. The average crystallite size of the Fe_3O_4 nanoparticles, calculated using Scherrer Eq (1):

$$D = \frac{0.9\lambda}{\beta \cos\theta} \quad (1)$$

Where, D is the average crystallite size, λ is the wavelength of X-ray radiation, β is the full width at half the maximum height (rad) and θ is the Bragg's angle in degree. The calculated average crystallite size from (311) diffraction peak is about 3 nm.

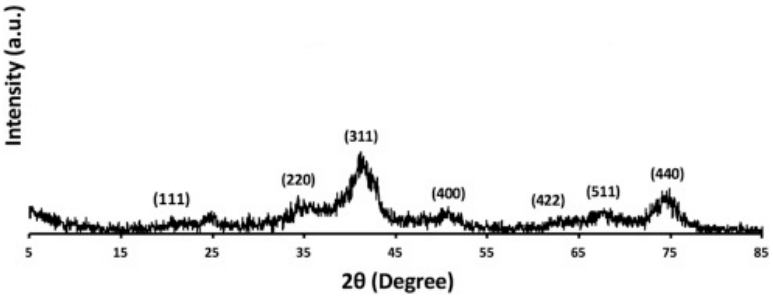

Fig. 1. XRD pattern of the synthezied Fe_3O_4 nanoparticles.

The FTIR spectrum (see Fig. 2a) displays the major peaks related to pure PVA. The absorption band at 3433.98 cm^{-1} is attributed to the stretching of O-H, 2921.68 cm^{-1} peak is related to the symmetric stretching of CH_2, 1714.24 cm^{-1} peak is due to carbonyl groups and 1660.66 cm^{-1} peak is assigned to the symmetric stretching of carboxylate anion (-COO-). The peak at 1444.67 cm^{-1} corresponds to the O-H and C-H bending. The band at 1103.16 cm^{-1} can be attributed to the C-O stretching and O-H bending vibrations.[40,44,45]

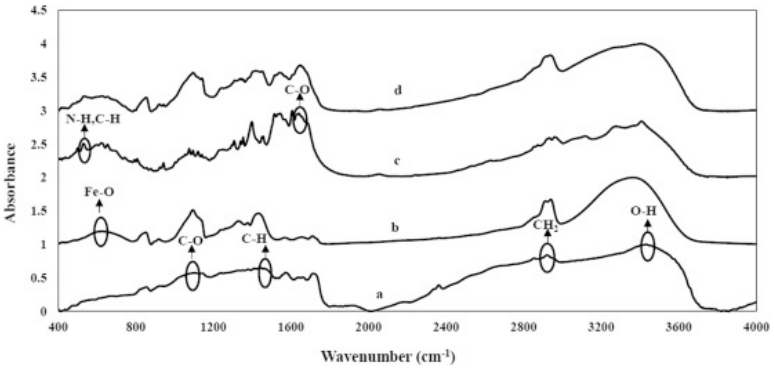

Fig. 2. FTIR spectra of (a) PVA, (b) PVA-Fe_3O_4 nanocomposite, (c) GOx and (d) GOx/PVA-Fe_3O_4 nanocomposite.

The FTIR spectrum of PVA-Fe_3O_4 nanocomposite is represented in Fig. 2b. The absorption band at 629.44 cm^{-1} is associated with the Fe-O stretching vibration and torsional vibration in the tetrahedral and octahedral sites.[17] These results indicate that the Fe_3O_4 nanoparticles are presented in PVA film. Fig. 2b obviously reveals the characteristic absorption bands of PVA and Fe_3O_4 nanoparticles.

The FTIR spectra of GOx and GOx/PVA-Fe_3O_4 nanocomposite are shown in Fig. 2c and d, respectively. Two major IR absorption bands related to amide I and II have been extensively used for characterization of GOx. The amide I absorption band appears at 1640.29 cm^{-1} belonging to the C-O stretching vibration in the protein's backbone. The band at 564.10 cm^{-1} exhibits the characteristics of N-H bending and C-N stretching of amid II.[46] The FTIR spectrum of the GOx/PVA-Fe_3O_4 nanocomposite shows characteristic absorption bands of GOx and PVA-Fe_3O_4 nanocomposite. Amide I and II IR bands are also observed in the spectrum of GOx/PVA-Fe_3O_4 nanocomposite. However, the peaks that correspond to functional groups of GOx and PVA-Fe_3O_4 nanocomposite overlap, thus the IR peaks shape become broader.

The morphology of PVA/Sn film, PVA-Fe_3O_4/Sn electrode and GOx/PVA-Fe_3O_4/Sn bioelectrode were characterized by FE-SEM (see Fig. 3). As shown in Fig. 3a the surface of PVA film seems very smooth, with no cracks or pores. As it was said, the average crystallite size of synthesized Fe_3O_4 nanoparticles is about 3 nm (according to Scherrer equation). Such small nanoparticles joined together and formed large aggregates, in order to minimize their surface energy. Fig. 3b shows that the Fe_3O4 nanoparticles created small aggregates, after dispersing in PVA matrix. In fact, PVA matrix somehow reduced the aggregates of magnetite nanoparticles. It can be seen from this figure, the surface of PVA- Fe_3O_4 nanocomposite is granular, due to the presence of magnetite nanoparticles. Small size of the magnetite nanoparticles (high surface to volume ratio) is beneficial for immobilization

of biomolecules. After the enzyme was immobilized on the PVA-Fe_3O_4 nanocomposite, the surface morphology has changed (Fig. 3c). It seems that the enzyme molecules were absorbed uniformly on the surface of PVA-Fe_3O_4 nanocomposite, so we can conclude that the enzyme molecules were successfully immobilized on the surface of this nanocomposite.

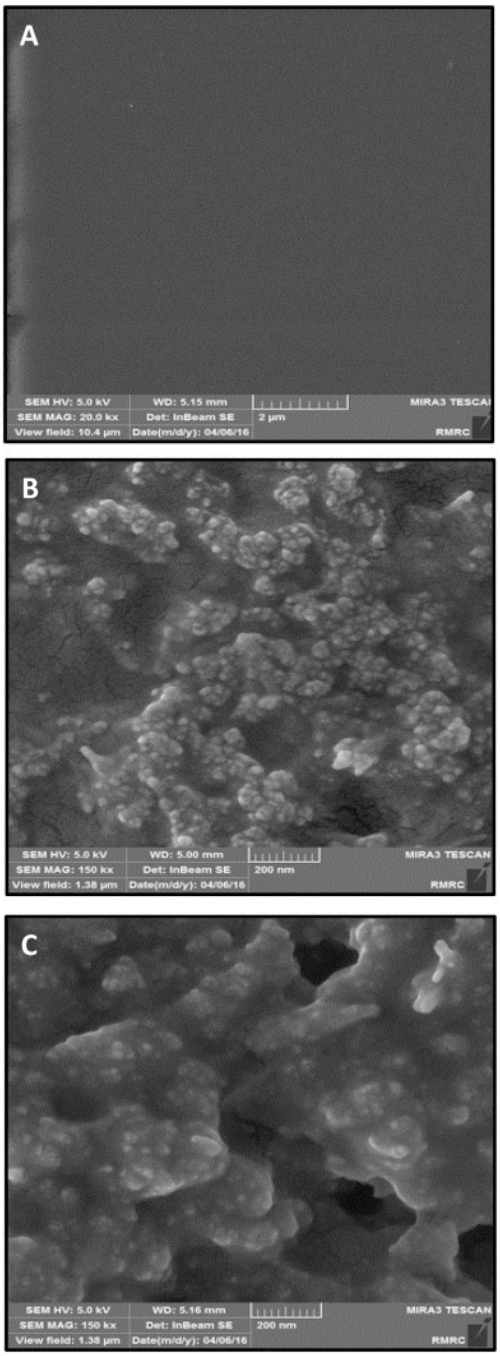

Fig. 3. FE-SEM micrographs of (a) PVA, (b) PVA-Fe_3O_4 nanocomposite and (c) GOx/PVA-Fe_3O_4 on Sn electrode.

3.2. Electrochemical impedance spectroscopic characterization of the electrodes

The PVA/Sn film, PVA-Fe_3O_4/Sn electrode and GOx/PVA-Fe_3O_4/Sn bioelectrode were monitored by EIS, which is a useful method to understand the features of the electrode surface. The linear part in the Nyquist plot of impedance spectra corresponds to the diffusion process. The semicircle part represents the electron-transfer limited process and its diameter is equal to the electron-transfer resistance, $R_{et,}$ which controls the electron transfer kinetics of the electrode interface. Fig. 4 exhibits the Nyquist plots of the EIS of PVA/Sn, PVA-Fe_3O_4/Sn electrode and GOx/PVA-Fe_3O_4/Sn bioelectrode in phosphate buffer (pH = 7) in the frequency range, 0.01–10^5 Hz. The largest semicircle diameter is related to the PVA/Sn film, indicating that PVA film is formed on the electrode surface and act as an insulating layer. The semicircle diameter of PVA-Fe_3O_4 nanocomposite (curve b) is smaller than that of PVA/Sn film (curve a), which suggests that the presence of Fe_3O_4 nanoparticles can act as a nanoscale electrode and facilitate the electron transfer between the electrolyte and electrode. However, after immobilization of GOx on PVA-Fe_3O_4 nanocomposite, the semicircle diameter increased. This suggest that GOx molecules are successfully assembled on the surface of PVA-Fe_3O_4 nanocomposite, which increase the electrode resistance and hinder the electron transfer between the electrolyte solution and electrode surface.

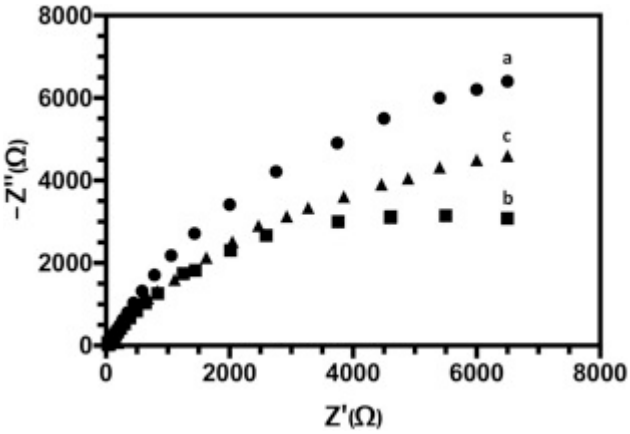

Fig. 4. EIS of (a) PVA/Sn film, (b) PVA-Fe_3O_4/Sn electrode and (c) GOx/PVA-Fe_3O_4/Sn bioelectrode.

3.3. Electrochemical behavior of the modified electrodes

To evaluate the electrochemical characteristics of the modified electrodes, the cyclic voltammetry technique is utilized. Fig. 5 illustrates the cyclic voltammograms of PVA/Sn film, PVA-Fe_3O_4/Sn electrode and GOx/PVA-Fe_3O_4/Sn bioelectrode in phosphate buffer (pH = 7) at the scan rate of 50 mVs^{-1}. For the PVA/Sn electrode (curve a) the oxidation and reduction peaks are appeared at 0.07 and −0.19 V respectively. In this curve, the

oxidation peak has the minimum current, indicating the formation of PVA layer on the electrode surface, which can act as a barrier for electron transfer between electrolyte solution and the electrode. The incorporation of Fe_3O_4 nanoparticles on to PVA modified Sn electrode surface leads to increase in peak current. This may be assigned to the properties of Fe_3O_4 nanoparticles, which can act as an electron transfer between the enzyme and electrode. However, after immobilization of GOx onto PVA-Fe_3O_4 electrode the peak current is found to increase remarkably. This improved peak current is attributed to the redox characteristics of active sites of the immobilized GOx, which promotes the electron transfer between GOx and electrode.

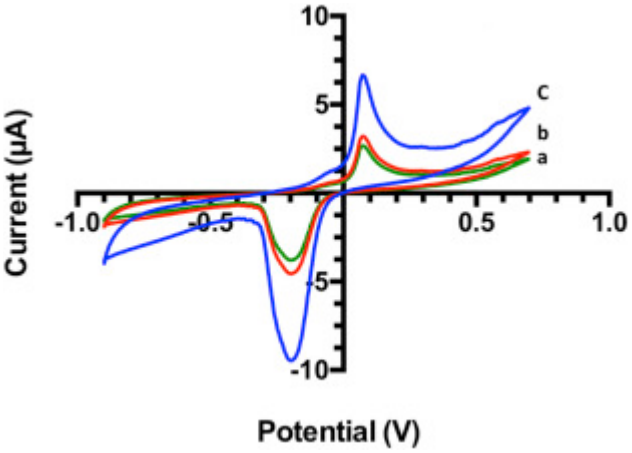

Fig. 5. CVs of (a) PVA, (b) PVA-Fe_3O_4/Sn electrode and (c) GOx/PVA-Fe_3O_4/Sn bioelectrode.

3.4. Effect of scan rate

The CVs of the GOx/PVA-Fe_3O_4/Sn bioelectrode in PBS (pH 7) over the potential range from −0.9 to 0.7 V with different scan rates are exhibited in Fig. 6. As can be seen, both the oxidation and reduction peaks current are increased linearly with increasing scan rates in the range from 10 to 400 mVs^{-1} with linear correlation coefficient 0.9899, which is shown in the inset of Fig. 6. The peak-to-peak separation (ΔE) has not changed by increasing the scan rates from 10 to 400 mVs^{-1} and it is almost independent of the scan rates, indicating that Fe_3O_4 nanoparticles can transfer electrons relatively fast and reversibly in this composite film. These results show that PVA-Fe_3O_4 nanocomposite can provide enough accessibility to electrons to transfer between the enzyme and the electrode. As a result, this nanocomposite can be employed for the immobilization of GOx.

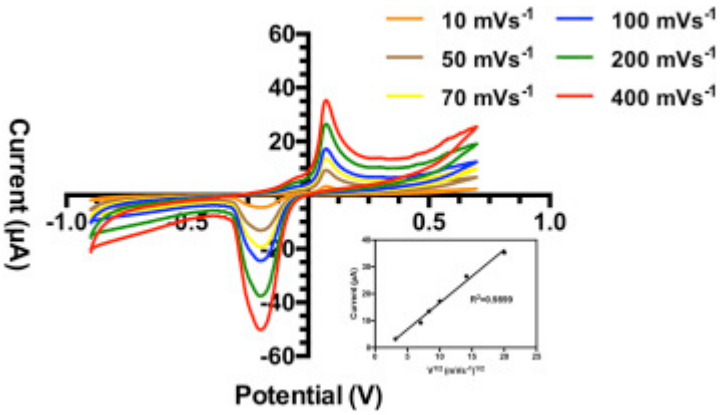

Fig. 6. CVs of GOx/PVA-Fe_3O_4/Sn bioelectrode at different scan rates. Inset: plot of current vs. $V^{1/2}$.

3.5. Optimization of experimental variables

3.5.1. Effect of enzyme concentration on the current response of the biosensor

The current response of glucose biosensor can be affected by the amount of GOx loading. Fig. 7 represents the effect of GOx concentration on the performance of the glucose biosensor. The result shows that the current response increases with the increasing of GOx loading for 5 mM glucose concentration. As can be seen, the peak current is saturated, when GOx concentration is more than 4 mg mL^{-1}. Thus, the optimal concentration of GOx for the biosensor is chosen 4 mg mL^{-1}.

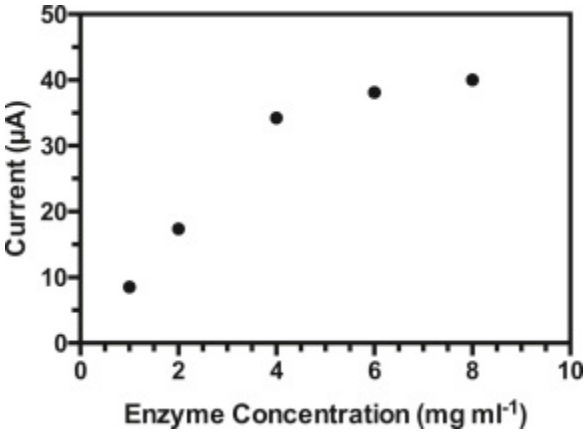

Fig. 7. Effect of different amounts of enzyme concentration on the current response.

3.5.2. Effect of pH on the current response of the biosensor

The effect of pH value on the performance of the biosensor is important because the enzymatic activity is affected by pH value. Fig. 8 shows the amperometric response of

GOx/PVA-Fe_3O_4/Sn bioelectrode at different pH values. It can be seen, the current response is increased with the increase of pH from 4 to 7 and the maximum current is obtained at pH = 7, then decreased at higher pH. The enzyme will be denatured in strong acidic or alkaline conditions, therefore pH = 7 is chosen as an optimum for the following study.

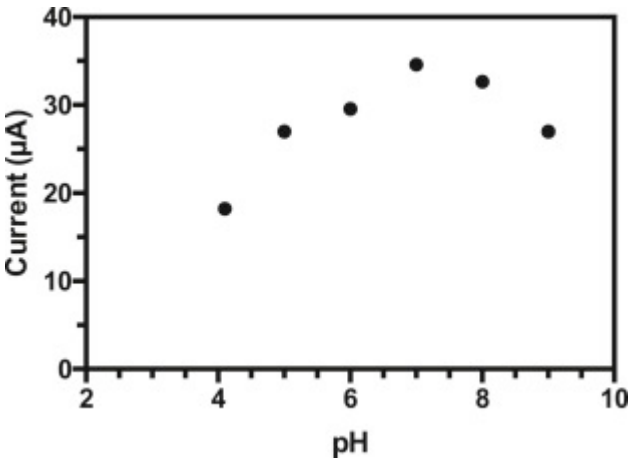

Fig. 8. Effect of pH value on the current response.

3.6. Electrochemical response of GOx/PVA-Fe_3O_4/Sn bioelectrode to glucose

Cyclic voltammetry responses of GOx/PVA-Fe_3O_4/Sn bioelectrode with GOx concentration of 4 mg mL^{-1} in different glucose concentrations in PBS buffer (pH = 7) at scan rate of 50 mVs^{-1} are illustrated in Fig. 9. As can be seen, there are no H_2O_2 redox peaks in the CV measurements. This may be related to the composite of PVA and Fe_3O_4 nanoparticles, which can accept electrons better than oxygen from the reduced enzyme. After enzymatic reaction, the GOx re-oxidized and the PVA-Fe_3O_4 nanocomposite film accepts electrons, therefore causing increases in the redox peaks of PVA-Fe_3O_4 nanocomposite. The redox current peaks are increased with increasing the glucose concentration. The GOx/PVA-Fe_3O_4/Sn bioelectrode has the response time of 10 s, which is related to the fast electron transfer characteristic of PVA-Fe_3O_4 nanocomposite.

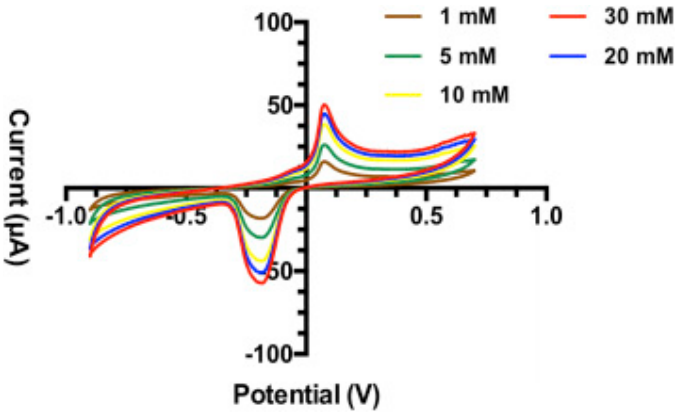

Fig. 9. CVs of GOx/PVA-Fe_3O_4/Sn bioelectrode in different glucose concentration.

Fig. 10 displays the glucose calibration plot in the range of 5×10^{-3} to 30 mM. The linear part of the calibration curve in the range of 5×10^{-3} -2 mM with correlation coefficient of 0.993 shows that the GOx/PVA-Fe_3O_4/Sn bioelectrode has well performance in glucose solution with a sensitivity of 9.36 μA mM^{-1}. The sensitivity of this bioelectrode is higher than those reported in previous literatures.[25,32] The limit of detection (LOD) was calculated using the following equation (2):

$$LOD = \frac{K \times S}{m} \quad (2)$$

Where K is the signal-to-noise ratio, S is the standard deviation of y-residuals of regression line and m is the slope of the linear plot. Signal-to-noise ratio is usually chosen to be 2 or 3, which 2 is related to a confidence level of 92.1% and 3 is related to a confidence level of 98.3%.[47] LOD was calculated to be 8 μM at a signal-to-noise ratio of 3 and the standard deviation of y-residuals of 24.96 nA with confidence limits of 13.27 ± 3.89. The LOD is lower than those calculated in previous reports.[25,48] The Michaelis-Menten constant (K_m) was calculated from the Lineweaver-Burk equation (3):

$$1/I_{ss} = (K_m/I_{max})(1/C) + 1/I_{max} \quad (3)$$

Where I_{ss} is the steady-state current, K_m is the Michaelis-Menten constant, I_{max} is the maximum current of the reaction and C is the concentration of the substrate. K_m was obtained to be 1.42 mM and I_{max} was 49.9 μA. The calculated K_m is lower than GOx/gold-platinum alloy nanoparticles/carbon nanotubes/chitosan (5.2 mM),[49] chitosan-

ferrocene/graphene oxide/GOx (2.1 mM)[50] and GOx immobislized on the ZnO nanotubes (19 mM).[51] It could be concluded that the modified biosensor has higher affinity to glucose.

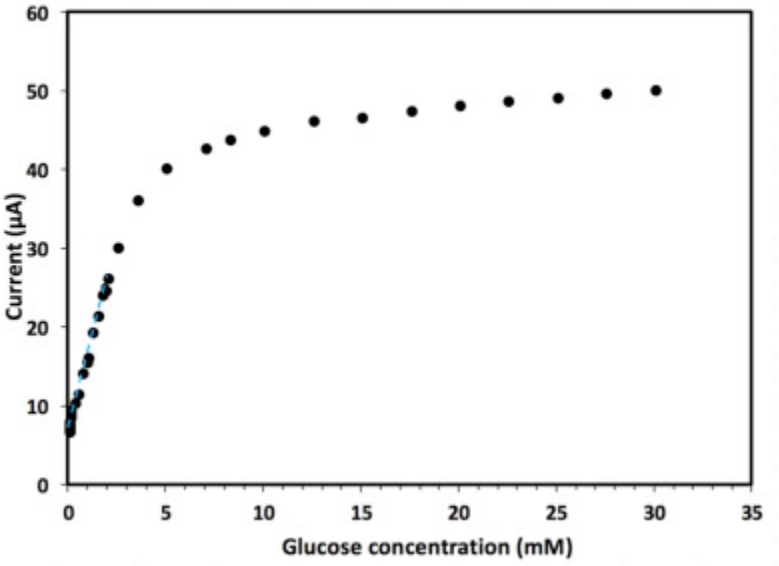

Fig. 10. Calibration curve of GOx/PVA-Fe_3O_4/Sn bioelectrode in the glucose range of 5×10^{-3} to 30 mM.

3.7. Reproducibility and stability of the modified biosensor

The reproducibility of the glucose biosensor is investigated by monitoring the current response of 5 GOx/PVA-Fe_3O_4/Sn bioelectrode samples in the presence of 5 mM glucose as shown in Table 1. The relative standard deviation (RSD) was calculated using the following equation (4):

$$\mathrm{RSD}(\%) = \frac{\text{Standard deviation}}{\text{Average}} \times 100 \quad (4)$$

Table 1. The current response of 5 GOx/PVA-Fe_3O_4/Sn bioelectrode in the presence of 5 mM glucose.

Sample	Current (μA)
1	30.24
2	28.31
3	31.68
4	30.95
5	28.81

The standard deviation, average and RSD were calculated as 1.269, 29.998 and 4.2%, respectively. The RSD was 4.2%, indicating the good reproducibility of the modified

enzyme electrode. The modified electrode was kept at 4 °C in PBS when not in used. The current response of biosensor is maintained about 81% of its initial response after a month. The results are suggesting that good stability of biosensor could be attributed to the Fe_3O_4 nanoparticles, which can provide biocompatible environment for immobilization of GOx and stabilize the enzyme bioactivity.[1,17]

3.8. Interference studies at GOx/PVA-Fe_3O_4/Sn bioelectrode

Fig. 11 shows the effect of different interferents including 0.2 mM uric acid (UA), 0.1 mM ascorbic acid (AA) and 2.5 mM cholesterol with glucose (5 mM) on the GOx/PVA-Fe_3O_4/Sn bioelectrode in phosphate buffer (pH 7) solution. The obtained results indicate that the addition of UA and AA do not cause significant change in current response for the detection of glucose. However, decrease of the peak current for cholesterol in glucose biosensor is observed. It could be concluded that the GOx/PVA-Fe_3O_4/Sn modified electrode displays good anti-interfering ability for the glucose detection.

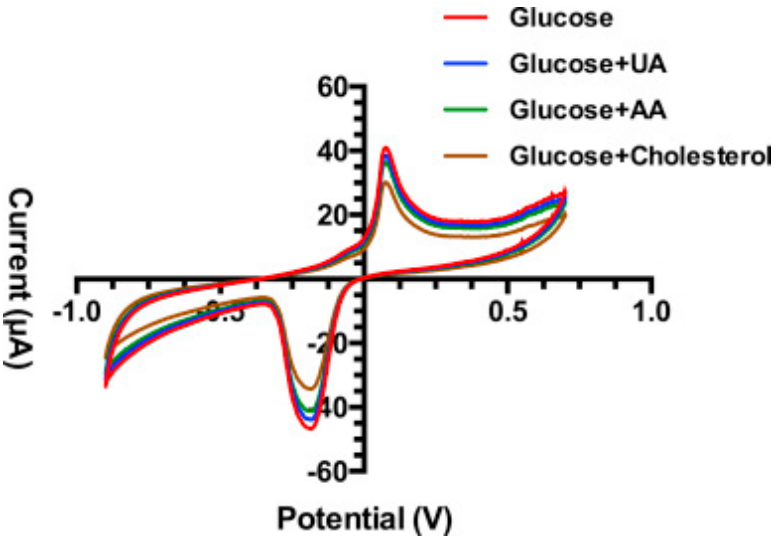

Fig. 11. The effect of interference on the GOx/PVA-Fe_3O_4/Sn bioelectrode.

4. Conclusions

We have presented a novel glucose biosensor using PVA-Fe_3O_4 nanocomposite as an ideal matrix for GOx entrapment. The dispersion of Fe_3O_4 nanoparticles in PVA matrix not only promote electron transfer between enzyme and electrode, but also provide a biocompatible environment for enzyme immobilization. The GOx/PVA-Fe_3O_4/Sn bioelectrode performed good electrocatalytic activity with a wide linearity, high sensitivity and low detection limit. In addition, the modified biosensor displayed good anti-interfering

capability toward glucose detection, fast response, good reproducibility and satisfactory stability. Finally, the investigations ascertained that the GOx/PVA-Fe_3O_4/Sn bioelectrode has great potential for the construction of biosensors.

References

[1]L. Yang, X. Ren, F. Tang, L. Zhang **A practical glucose biosensor based on Fe 3 O 4 nanoparticles and chitosan/nafion composite film** *Biosens. Bioelectron.*, 25 (2009), pp. 889-895

[2]J. Lin, C. He, Y. Zhao, S. Zhang **One-step synthesis of silver nanoparticles/carbon nanotubes/chitosan film and its application in glucose biosensor** *Sensors Actuators B Chem.*, 137 (2009), pp. 768-773

[3]B. Bahmani, F. Moztarzadeh, M. Rabiee, M. Tahriri **Development of an electrochemical sulfite biosensor by immobilization of sulfite oxidase on conducting polyaniline film** *Synth. Met.*, 160 (2010), pp. 2653-2657

[4]S. Yazdanpanah, M. Rabiee, M. Tahriri, M. Abdolrahim, L. Tayebi **Glycated hemoglobin-detection methods based on electrochemical biosensors** *TrAC Trends Anal. Chem.*, 72 (2015), pp. 53-67

[5]B. Bahmani, F. Moztarzadeh, M. Hossini, M. Rabiee, M. Tahriri, M. Rezvannia, *et al.*" **A sulfite biosensor fabricated by immobilization of sulfite oxidase on aluminum electrode modified with electropolymerized conducting film (polyaniline)** *Asian J. Chem.*, 21 (2009), p. 923

[6]M. Abdorahim, M. Rabiee, S.N. Alhosseini, M. Tahriri, S. Yazdanpanah, S.H. Alavi, *et al.* **Nanomaterials-based electrochemical immunosensors for cardiac troponin recognition: an illustrated review** *TrAC Trends Anal. Chem.*, 82 (2016), pp. 337-347

[7]X. Chen, J. Zhu, Z. Chen, C. Xu, Y. Wang, C. Yao **A novel bienzyme glucose biosensor based on three-layer Au–Fe3O4@SiO2 magnetic nanocomposite** *Sensors Actuators B Chem.*, 159 (2011), pp. 220-228

[8]K. Xue, S. Zhou, H. Shi, X. Feng, H. Xin, W. Song **A novel amperometric glucose biosensor based on ternary gold nanoparticles/polypyrrole/reduced graphene oxide nanocomposite** *Sensors Actuators B Chem.*, 203 (2014), pp. 412-416

[9]S. Liu, H. Ju **Reagentless glucose biosensor based on direct electron transfer of glucose oxidase immobilized on colloidal gold modified carbon paste electrode** *Biosens. Bioelectron.*, 19 (2003), pp. 177-183

[10]M. Abdolrahim, M. Rabiee, S.N. Alhosseini, M. Tahriri, S. Yazdanpanah, L. Tayebi **Development of optical biosensor technologies for cardiac troponin recognition** *Anal. Biochem.*, 485 (2015), pp. 1-10

[11]E. Mohagheghpour, M. Rabiee, F. Moztarzadeh, M. Tahriri, M. Jafarbeglou, D. Bizari, *et al.* **Controllable synthesis, characterization and optical properties of ZnS: Mn nanoparticles as a novel biosensor** *Mater. Sci. Eng. C,* 29 (2009), pp. 1842-1848

[12]E. Mohagheghpour, R. Salimi, H. Sameie, F. Moztarzadeh, M. Roohnikan, M.A.M. Farsi, *et al.* **A new optical bio-sensor: wet-chemical synthesis and surface treatment of nanocrystalline Zn 1-x S: Mn+ 2 x** *Opt. Sensors* (2011), p. SWC4

[13]M. Alizadeh, R. Salimi, H. Sameie, A.A. Sarabi, A.A. Sabbagh Alvani, M. Tahriri **The wet-chemical synthesis of functionalized Zn1–xOMnx quantum dots utilizable in optical biosensors** *Materiali tehnologije*, 47 (2013), pp. 235-237

[14]M. Tayebi, M.T. Yaraki, A. Mogharei, M. Ahmadieh, M. Tahriri, D. Vashaee, *et al.* **Thioglycolic acid-capped CdS quantum dots conjugated to α-amylase as a fluorescence probe for determination of starch at low concentration** *J. Fluoresc.* (2016), pp. 1-8

[15]M. Tayebi, M.T. Yaraki, M. Ahmadieh, M. Tahriri, D. Vashaee, L. Tayebi **Determination of total aflatoxin using cysteamine-capped CdS quantum dots as a fluorescence probe** *Colloid Polym. Sci.* (2016), pp. 1-10

[16]M. Tayebi, M.T. Yaraki, M. Ahmadieh, A. Mogharei, M. Tahriri, D. Vashaee, *et al.* **Synthesis, surface modification and optical properties of thioglycolic acid-capped ZnS quantum dots for starch recognition at ultralow concentration** *J. Electron. Mater.* (2016), pp. 1-8

[17]A. Kaushik, R. Khan, P.R. Solanki, P. Pandey, J. Alam, S. Ahmad, *et al.* **Iron oxide nanoparticles–chitosan composite based glucose biosensor** *Biosens. Bioelectron.*, 24 (2008), pp. 676-683

[18]K.J. Cash, H.A. Clark **Nanosensors and nanomaterials for monitoring glucose in diabetes** *Trends Mol. Med.*, 16 (Dec 2010), pp. 584-593

[19]A. Chen, S. Chatterjee **Nanomaterials based electrochemical sensors for biomedical applications** *Chem. Soc. Rev.*, 42 (Jun 21 2013), pp. 5425-5438

[20]H. Ju, X. Zhang, J. Wang *NanoBiosensing: Principles, Development and Application* Springer Science & Business Media (2011)

[21]S. Zeng, K.-T. Yong, I. Roy, X.-Q. Dinh, X. Yu, F. Luan **A review on functionalized gold nanoparticles for biosensing applications** *Plasmonics*, 6 (2011), pp. 491-506

[22]J.M. Pingarrón, P. Yáñez-Sedeño, A. González-Cortés **Gold nanoparticle-based electrochemical biosensors** *Electrochimica Acta*, 53 (2008), pp. 5848-5866

[23]R. Rawal, S. Chawla, C.S. Pundir **"Polyphenol biosensor based on laccase immobilized onto silver nanoparticles/multiwalled carbon nanotube/polyaniline gold electrode** *Anal. Biochem.*, 419 (Dec 15 2011), pp. 196-204

[24]Z. Chang, H. Fan, K. Zhao, M. Chen, P. He, Y. Fang **"Electrochemical DNA biosensors based on palladium nanoparticles combined with carbon nanotubes** *Electroanalysis*, 20 (2008), pp. 131-136

[25]X. Jiang, Y. Wu, X. Mao, X. Cui, L. Zhu **Amperometric glucose biosensor based on integration of glucose oxidase with platinum nanoparticles/ordered mesoporous carbon nanocomposite** *Sensors Actuators B Chem.*, 153 (2011), pp. 158-163

[26]H. Wu, J. Wang, X. Kang, C. Wang, D. Wang, J. Liu, *et al.* **Glucose biosensor based on immobilization of glucose oxidase in platinum nanoparticles/graphene/chitosan nanocomposite film** *Talanta*, 80 (Nov 15 2009), pp. 403-406

[27]N. Chauhan, C.S. Pundir **An amperometric biosensor based on acetylcholinesterase immobilized onto iron oxide nanoparticles/multi-walled carbon nanotubes modified gold electrode for measurement of organophosphorus insecticides** *Anal. Chim. Acta*, 701 (Sep 2 2011), pp. 66-74

[28]Y. Du, X.L. Luo, J.J. Xu, H.Y. Chen **A simple method to fabricate a chitosan-gold nanoparticles film and its application in glucose biosensor** *Bioelectrochemistry*, 70 (May 2007), pp. 342-347

[29]Y. Xing, Y.-Y. Jin, J.-C. Si, M.-L. Peng, X.-F. Wang, C. Chen, *et al.* **Controllable synthesis and characterization of Fe3O4/Au composite nanoparticles** *J. Magnetism Magnetic Mater.*, 380 (2015), pp. 150-156

[30]G.-S. Lai, H.-L. Zhang, D.-Y. Han **Amperometric hydrogen peroxide biosensor based on the immobilization of horseradish peroxidase by carbon-coated iron nanoparticles in combination with chitosan and cross-linking of glutaraldehyde** *Microchim. Acta*, 165 (2008), pp. 159-165

[31]J. Li, H. Gao **A renewable potentiometric immunosensor based on Fe3O4 nanoparticles immobilized anti-IgG** *Electroanalysis*, 20 (2008), pp. 881-887

[32]B.-W. Lu, W.-C. Chen **A disposable glucose biosensor based on drop-coating of screen-printed carbon electrodes with magnetic nanoparticles** *J. magnetism magnetic Mater.*, 304 (2006), pp. e400-e402

[33]M. Rieth World Scientific *Nano-engineering in Science and Technology*, vol. 20 (2003)

[34]J. Kumar, S.F. D'Souza **Preparation of PVA membrane for immobilization of GOD for glucose biosensor** *Talanta*, 75 (Mar 15 2008), pp. 183-188

[35]S. Shukla, S.R. Deshpande, S.K. Shukla, A. Tiwari **Fabrication of a tunable glucose biosensor based on zinc oxide/chitosan-graft-poly (vinyl alcohol) core-shell nanocomposite** *Talanta*, 99 (2012), pp. 283-287

[36]Y. Xin, X. Fu-bing, L. Hong-wei, W. Feng, C. Di-zhao, W. Zhao-yang **A novel H 2 O 2 biosensor based on Fe 3 O 4–Au magnetic nanoparticles coated horseradish peroxidase and graphene sheets–Nafion film modified screen-printed carbon electrode** *Electrochimica Acta*, 109 (2013), pp. 750-755

[37]S. Masoomi-Godarzi, A. Khodadadi, M. Vesali-Naseh, Y. Mortazavi **Highly stable and selective non-enzymatic glucose biosensor using carbon nanotubes decorated by Fe3O4 nanoparticles** *J. Electrochem. Soc.*, 161 (2014), pp. B19-B25

[38]Z. Yang, C. Zhang, J. Zhang, W. Bai **Potentiometric glucose biosensor based on core–shell Fe 3 O 4–enzyme–polypyrrole nanoparticles** *Biosens. Bioelectron.*, 51 (2014), pp. 268-273

[39]S. Tan, X. Tan, J. Jiang, J. Xu, J. Zhang, D. Zhao, *et al.* **Hydrogen peroxide biosensor based on poly (vinyl alcohol)/ZnO nanorods composite films** *J. Electroanal. Chem.*, 668 (2012), pp. 113-118

[40]U. Lad, G.M. Kale, R. Bryaskova **Glucose oxidase encapsulated polyvinyl alcohol–silica hybrid films for an electrochemical glucose sensing electrode** *Anal. Chem.*, 85 (2013), pp. 6349-6355

[41]Y. Fang, D. Zhang, X. Qin, Z. Miao, S. Takahashi, J.-i. Anzai, *et al.* **A non-enzymatic hydrogen peroxide sensor based on poly (vinyl alcohol)–multiwalled carbon nanotubes–platinum nanoparticles hybrids modified glassy carbon electrode** *Electrochimica Acta*, 70 (2012), pp. 266-271

[42]Y.S. Kang, S. Risbud, J.F. Rabolt, P. Stroeve **Synthesis and characterization of nanometer-size Fe3O4 and γ-Fe2O3 particles** *Chem. Mater.,* 8 (1996), pp. 2209-2211

[43]R. Hachani, M. Lowdell, M. Birchall, A. Hervault, D. Mertz, S. Begin-Colin, *et al.* **Polyol synthesis, functionalisation, and biocompatibility studies of superparamagnetic iron oxide nanoparticles as potential MRI contrast agents** *Nanoscale*, 8 (2016), pp. 3278-3287

[44]C.-M. Tang, Y.-H. Tian, S.-H. Hsu **Poly (vinyl alcohol) nanocomposites reinforced with bamboo charcoal nanoparticles: mineralization behavior and characterization** *Materials*, 8 (2015), pp. 4895-4911

[45]N. Labidi, A. Djebaili **Studies of the mechanism of polyvinyl alcohol adsorption on the calcite/water interface in the presence of sodium oleate** *J. Minerals Mater. Charact. Eng.*, 7 (2008), p. 147

[46]E.F.d. Reis, F.S. Campos, A.P. Lage, R.C. Leite, L.G. Heneine, W.L. Vasconcelos, *et al.* **Synthesis and characterization of poly (vinyl alcohol) hydrogels and hybrids for rMPB70 protein adsorption** *Mater. Res.*, 9 (2006), pp. 185-191

[47]D.A. Skoog, D.M. West, F.J. Holler, S.R. Crouch *Fundamentals of Analytical Chemistry* Nelson Education (2013)

[48]Y. Du, X.-L. Luo, J.-J. Xu, H.-Y. Chen **A simple method to fabricate a chitosan-gold nanoparticles film and its application in glucose biosensor** *Bioelectrochemistry*, 70 (2007), pp. 342-347

[49]X. Kang, Z. Mai, X. Zou, P. Cai, J. Mo **A novel glucose biosensor based on immobilization of glucose oxidase in chitosan on a glassy carbon electrode modified with gold–platinum alloy nanoparticles/multiwall carbon nanotubes** *Anal. Biochem.*, 369 (2007), pp. 71-79

[50]J.-D. Qiu, J. Huang, R.-P. Liang **Nanocomposite film based on graphene oxide for high performance flexible glucose biosensor** *Sensors Actuators B Chem.*, 160 (2011), pp. 287-294

[51]T. Kong, Y. Chen, Y. Ye, K. Zhang, Z. Wang, X. Wang **An amperometric glucose biosensor based on the immobilization of glucose oxidase on the ZnO nanotubes** *Sensors Actuators B Chem.*, 138 (2009), pp. 344-350